Self-Organization of a Carbide Superlattice during Deposition of Carbon on Mo

F. Tsui* and P. A. Ryan

Department of Physics and Astronomy, University of North Carolina, Chapel Hill, North Carolina 27599

(Received 23 January 2002; published 18 June 2002)

Formation and evolution of a carbide superlattice (SL) during C deposition on Mo have been studied using molecular beam epitaxy techniques. The ordering of the SL is energetically driven, such that the interplay between strain and surface energies determines the length scale of the SL. Surface precipitation of C occurs within a narrow range of SL spacing that appears to control the size and spacing of the precipitates leading to a possible mechanism for nucleation of single-walled carbon nanotubes.

DOI: 10.1103/PhysRevLett.89.015503 PACS numbers: 68.35.–p, 61.46.+w, 68.55.Ac, 81.15.Hi

Formation of carbides in transition metals has long been a subject of interest since the Industrial Revolution. Recently, many of the same transition metals have been used as catalysts for the production of single-walled carbon nanotubes (SWNT) [1]. The low dimensional nature of SWNT and the potential for applications have caused a great deal of excitement. The subject of nanoscale ordering and interactions between metal and C has come to the forefront of scientific research. Knowledge and understanding of these phenomena are critically important for controlling synthesis and properties and for device applications. Despite the great strides made in synthesizing SWNT using numerous techniques, such as arc discharge [2,3], laser ablation [4], and chemical vapor deposition [5], and in characterizing their physical properties, the mechanisms by which they nucleate and grow from metal catalysts are still under great debate. One of the main reasons for the controversy is that the growth techniques currently employed, though very successful in producing high quality materials, by and large do not lend themselves to direct *in situ* characterization, so the exact role of the metal catalyst, which is required for the growth of SWNT, and its interaction with C have not been determined. In this Letter, we report direct observation of self-organization and evolution of a carbide superlattice (SL) during deposition of C on Mo, a known SWNT catalyst [6], using molecular beam epitaxy (MBE) techniques. Epitaxially grown Mo ultrathin films on sapphire substrates were used as templates for C deposition. The key reasons for choosing this approach for the study are the available *in situ* characterization techniques, particularly for real-time diffraction experiments using reflection high-energy electron diffraction (RHEED) and the ability to produce controlled surface orientations and morphology of the catalyst. The observed structural evolution as a function of temperature and C flux reveals evidence for a strain driven ordering and suggests a possible nucleation mechanism of SWNT.

The study was carried out using an advanced MBE system, equipped with a scanning RHEED imaging system and scanning tunneling microscopes (STM). The 30 keV RHEED beam can be scanned at a chosen azimuth across the sample and the patterns imaged in real time using a charge-coupled device camera, such that structural evolution across the substrate as a function of time can be explored systematically. Epitaxial growth of the Mo templates followed well-established procedures [7] with a set of chosen growth parameters to produce three-dimensional (3D) surfaces with correlated feature height and separation. The initial focus of the study was on the dependence of structures on C flux, and on substrate temperature and orientation. Various faces of Mo at a fixed thickness of $\sim$50 Å were used, including (111) and (110), which were determined by the orientations of the substrates. Controlled deposition rates between one and tens of atomic layers per minute (AL/min) for both Mo and C were produced by electron beam hearths, and substrate temperature varied between several hundred and 1200 °C. The base pressure of the system was 5×10^{-11} Torr, and the pressure during deposition was kept below 10^{-9} Torr. Analyses of the C flux using a mass spectrometer during deposition indicate that the main species from the *e*-beam hearth were C_1, C_2, and C_3, with C_3 being the most abundant. Traces of C_4 to C_8 were present also. The initial question clearly is: What happens to the C clusters when they land on the Mo surface?

Our real-time RHEED observations show that the initial deposition of C on Mo (111) leads to the formation of a SL of carbide nanocrystals in the growth plane of Mo. Such ordered structure is absent for deposition on other faces of Mo, including (110) and (112). In what follows, we describe the formation and evolution of the carbide SL in the (111) system. The observed behavior follows three distinct stages — initial formation of a SL, coarsening of the SL, and, finally, precipitation of C nanostructures — as they are illustrated in Fig. 1 by the RHEED intensities of the different structures for deposition at 1000 °C and flux of $\sim$1 AL/min. Beginning at C coverage of $<$0.1 AL (between *a* and *b* in Fig. 1), a new set of RHEED patterns in addition to those of Mo appears [Fig. 1(b)]. The additional patterns consist of features from an ordered carbide crystal and satellite peaks around them. As with all forms of diffraction, the observed satellites indicate that the carbide crystals form a regular array in the growth plane, i.e., a planar SL of carbide nanocrystals. The spacing of the SL

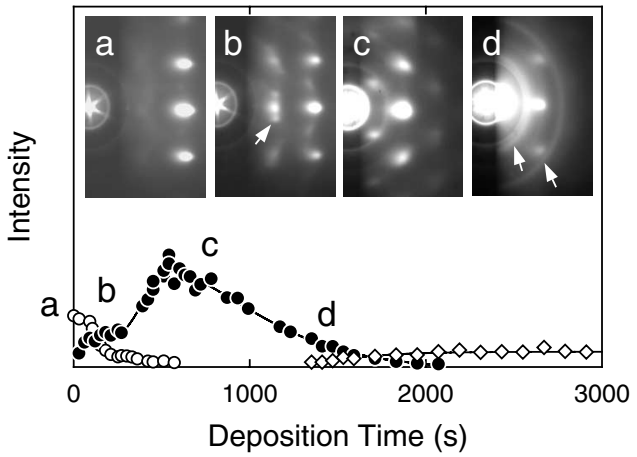

FIG. 1. Evolution of RHEED intensities of Mo (111) (open circles), carbide SL (closed circles), and C precipitate (diamonds) during deposition at 1000 °C and ~1 AL/min. Inset: RHEED patterns at various stages of the deposition along the [110] azimuth of Mo: (a) pure Mo (111), (b) mixed Mo (111) and SL, (c) SL, and (d) carbide and graphenelike precipitates. The letters on the graph indicate where the inset patterns were taken. Diffraction geometry with respect to the patterns: sample surface facing right, direct beam (000) left middle below the labels, Mo [111] along the horizontal, and Mo [110] vertical. To the right of (a) are the Mo spots across (222). The additional pattern in (b) corresponds to that of the carbide with the arrow indicating (002) and the satellites. In (c), carbide pattern intensifies and satellite spacing decreases. The rings in (d) indicated by arrows correspond to graphene (100) and (110).

is inversely proportional to that of the satellite peaks, and for the growth shown in Fig. 1 the initial spacing is about 10 Å along the in-plane Mo ⟨110⟩. As the RHEED intensity from the carbide increases with further deposition, the intensity from Mo decreases and the spacing between the satellite peaks also decreases. The reverse correlation in intensity shown in Fig. 1 between regions *b* and *c* indicates that the C species arriving at the surface are continuously absorbed into the Mo matrix to form more and more carbide. The observed change in satellite spacing, on the other hand, indicates that the continuous absorption of C leads to coarsening of the SL, i.e., increasing the separation between the carbide nanocrystals. Upon further deposition, the carbide RHEED intensity (region between *c* and *d* in Fig. 1) decreases, and subsequently polycrystalline C patterns [the rings in Fig. 1(d)] appear, signaling the precipitation of C on the surface. The C RHEED pattern can be indexed to the graphitic (100), (110), (200), (300), ... reflections with all of the (002) related reflections absent. This observation indicates that the C precipitates are either nanostructures of individual graphene sheets or the initial "nucleus" of SWNT, but there is perhaps no distinction between the two at this early stage. However, further deposition does not change the RHEED patterns qualitatively, which indicates that the growth condition with Mo as the catalyst does not favor formation of graphite nor multiwalled nanotubes, where spacing between graphene layers would give rise to intensities at (002) and related reflections. Before we further describe the structure and morphology of the precipitates, we continue to focus on the SL, particularly its evolution and origin.

Coarsening of the SL has been examined as a function of temperature and flux (in the range of one to tens of AL/min). The temperature dependent result for a flux of 1 AL/min is shown in Fig. 2. The initial SL spacing R_C appears to be independent of temperature and flux, indicating that it is an energetically driven phenomenon. As more C atoms are incorporated into the SL, R_C first increases linearly at each temperature [Fig. 2(a)] and flux, and then it saturates. An initial coarsening rate, r_c can be obtained from the linear behavior, which gives a quantitative measure of the initial process. The measured r_c increases with increasing temperature and decreasing flux, indicating the important role played by kinetics, specifically processes involving the detachment from small clusters arriving at the surface and the subsequent diffusion. As one would expect, the observed precipitation time also exhibits similar correlation. Further analysis of the temperature dependence indicates that r_c exhibits an Arrhenius relationship with activation energy ε_a of (0.7 ± 0.1) eV [Fig. 2(b)], and that the same ε_a is observed for different C rates within our experimental range. As mentioned above, the key processes involved in the evolution of the SL are detachment and diffusion, since C clusters do not diffuse as easily as atomic species on or into the Mo surface and no ordered C structures are observed at this stage of deposition. The observed low ε_a reveals unequivocally that one of the key roles played by Mo as a catalyst is to significantly reduce the energy required for breaking up C clusters, which has been predicted to cost several eV, particularly for small clusters [8]. It is also reasonable to conclude that the measured ε_a is controlled by diffusion processes. If detaching from clusters were to be the rate limiting process, low temperature deposition would lead

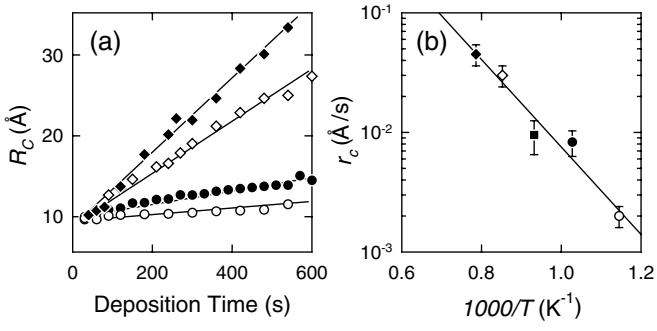

FIG. 2. (a) Initial coarsening of SL spacing R_C, as a function of deposition time for a C flux of 1 AL/min at various temperatures, 600 °C (open circles), 700 °C (closed circles), 900 °C (open diamonds), and 1000 °C (closed diamonds). Lines are linear fits of the data. (b) Arrhenius plot of coarsening rate, r_c, at the same flux of 1 AL/min. The line is a fit of the data with activation energy of (0.7 ± 0.1) eV.

to accumulation of C on the surface and, if this surface were to be annealed, coarsening would occur, as more C atoms are generated and incorporated into the SL. Such experiments involving low temperature growth followed by annealing at temperatures up to 1200 °C were carried out, and no additional coarsening was observed. Furthermore, since the energy for interstitial diffusion of C in bulk Mo is ~1.8 eV [9], the measured ε_a is thus dominated by surface and interfacial processes, particularly surface diffusion and diffusion around the boundaries of carbide crystals. These processes are further examined in what follows, particularly in the context of the origin of the self-organized structure.

Orientation dependent diffraction experiments show that both the carbide and SL are hexagonal in the Mo (111) plane, with the former being epitaxial and coherent in-plane and exhibiting a 3D epitaxial relationship with the Mo host, i.e., [002], [100], and [110] of the hexagonal carbide parallel to [222], [110], and [211] of bcc Mo, respectively. Further examination of the in-plane lattice spacings of both carbide and Mo reveals that they remain coherent at least initially [10], such that the Mo in-plane lattice expands with that of the carbide during the formation and coarsening processes. The in-plane Mo lattice spacing also appears to correlate with that of the SL. These observations strongly suggest that the origin of the observed structure lies in the strain of the system. Strain effects have been attributed to many self-organized surface phenomena [11]. Recent theoretical work [12] has shown that the chemical potential of surface islands under strain exhibit a minimum with respect to island radius $R_0 \sim \exp(\sigma/\alpha)$, and that island edge diffusion in addition to surface diffusion can give rise to an effective diffusion of islands leading to an energetically driven self-organized array of islands with both regular size and spacing while surface diffusion alone may instead lead to larger islands with kinetics dependent power-law size distributions. Here σ is related to surface energy, and α is related to strain and elastic properties. By symmetry, the model should be analogous to the near surface phenomenon reported here.

In order to test the strain dependence while maintaining surface chemistry, we studied C deposition on templates that contained buffer layers of other (111) bcc metals grown epitaxially between the substrate and the top Mo (111). Figure 3 (inset) illustrates the sample geometry using V and Nb wedges as the strain-tuning buffer layers, such that the in-plane Mo lattice spacing, d_{Mo}, were tuned continuously between −1% (compression) and +5% (expansion). The results shown in Fig. 3 confirm the presence of a correlation between the lattice spacings of the SL and Mo, hence establishing the strain dependence. The data in Fig. 3 were fitted to the form $R_{\mathrm{C}} = a_0 \exp[b/(\Delta d)^2]$, where Δd $(= d_{\mathrm{C}} - d_{\mathrm{Mo}})$ is the lattice mismatch between the carbide and Mo, and a_0 is related to a cutoff length and b is related to surface energy and elastic parameters [12].

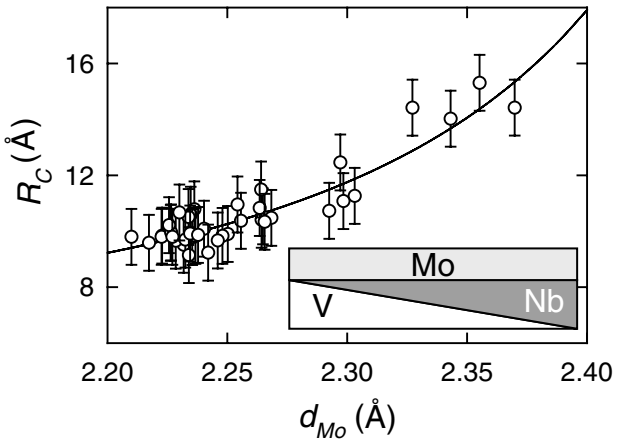

FIG. 3. Correlation of SL spacing R_{C} and Mo [110] spacing d_{Mo}. The line is a fit of the data using $R_{\mathrm{C}} = a_0 \exp[b/(d_{\mathrm{C}} - d_{\mathrm{Mo}})^2]$ [12], with $a_0 = 5.0$ Å, $b = 0.26$ Å^2, and $d_{\mathrm{C}} = 2.8 \pm 0.2$ Å. Inset: schematic diagram of the sample. The wedge-shaped layers were produced using motorized shadow masks during deposition.

Although the large uncertainty present in the data does not allow precise determination of various parameters that influence the self-organization process, nor does it show the uniqueness of the functional fit, the observed one-to-one correspondence nevertheless indicates that the origin of the SL arises from the competition between strain and surface energies. In other words, lattice mismatch between the carbide and Mo uniquely determines the SL spacing. Furthermore, the fact that d_{C} along [100] (2.8 ± 0.2 Å) from the fit is within uncertainty the same as those of many known hexagonal Mo_2C (2.6 Å) [13] perhaps lends more credence to the particular fit. From the above discussions, the most logical rate limiting process should be that of effective island diffusion, so the measured ε_a is likely to be associated with it. The observed increase in SL coherence length during coarsening, which is indicated by narrowing of the satellite widths, further supports this view.

It is interesting to point out that the symmetry and stacking sequence of the carbide are consistent with those of the interstitial Hägg phases (e.g., Mo_2C) [14], where the C atoms occupy the interstitial sites of Mo. The key difference for the observed carbide is that by occupying the interstitial sites the addition of C expands the Mo matrix by ~10% in the growth direction (Mo [111]), resulting in a carbide that is substantially smaller along the [002] (~20%) than that of an hcp Hägg phase, evidently owing to the preexistence of the Mo matrix. While these observations indicate the complex nature of the interfaces between the carbide and Mo containing both chemical and structural boundaries, the carbide nanocrystals themselves may be compact and may have atomically sharp interfaces with Mo, owing to the energetically driven processes, particularly phase separation and the minimum in chemical potential. Furthermore, the presence of a unique epitaxial arrangement in the (111) system and the absence in other

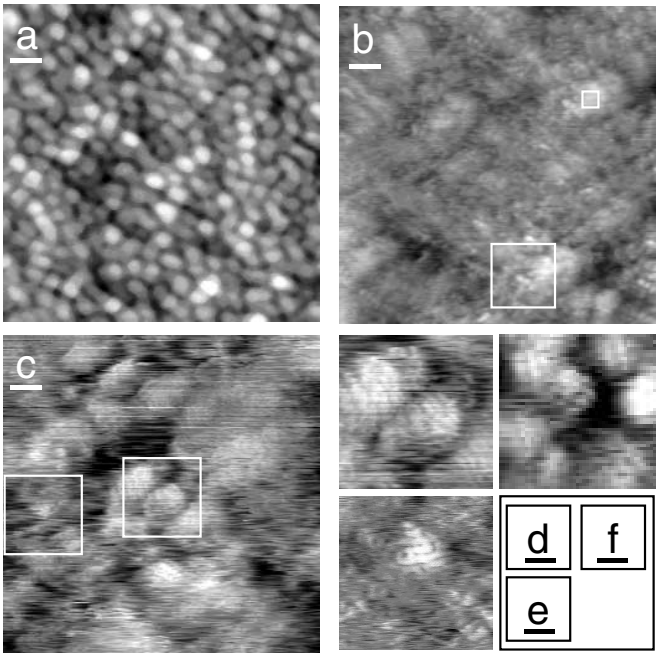

FIG. 4. STM images of (a) initial Mo (111), and (b)–(f) surfaces at the time of C precipitation for deposition at 800 °C. The lower right-hand box indicates the arrangement of (d)–(f). Image sizes are 1000 Å × 1000 Å for (a) and (b), 200 Å × 200 Å for (c), and 50 Å × 50 Å for (d) to (f). The z range for images are (a) 8 Å, (b) 12 Å, (c) 8 Å, and (d)–(f) 5 Å. The scale bars under each letter are (a) and (b) 100 Å, (c) 20 Å, and (d)–(f) 10 Å. The large and small boxes in (b) correspond to zoomed images of (c) and (f), respectively, and the two boxes in (c) correspond to (d) and (e). In addition to having characteristic "donutlike" features, the precipitates exhibit characteristic size and spacing with the latter being about 25 Å.

faces of Mo should be the reason for whether or not the SL can form.

Finally, we examine the structure and morphology of the C precipitates. Since precipitation on the surface occurs over a rather narrow range of SL spacing, one would expect that the graphenelike precipitates mimic the morphology of the SL. Our STM results shown in Fig. 4 for growth at 800 °C support this. During the initial stages of deposition until right before precipitation [close to Fig. 1(d)], no qualitative change on the surface was observed, when compared to that of the pristine Mo [Fig. 4(a)]. When precipitation occurs, surface morphology changes suddenly [Figs. 4(b)–4(f)]. The round Mo moundlike features disappear and they are replaced by a surface that is somewhat featureless at the long length scale but with small and regular dots on the short length scale. Higher resolution STM images [Figs. 4(d)–4(f)] show that the size, including the isolated ones [Fig. 4(e)], and separation of the graphene precipitate are rather regular and they appear to correlate with those of the SL. It is reasonable to expect that the precipitation occurs above the carbide nanocrystals instead of the space between them, and it perhaps terminates the coarsening process, since the C species are now beginning to be incorporated into surface structures. The observed precipitates show curvature similar to the end caps of SWNT, and have no apparent tendency to coalesce. This finding suggests that the carbide nanocrystals may be the "roots" for nucleating SWNT. It is widely believed that SWNT nucleate from catalysts with comparable size, and therefore this mechanism provides an alternative for larger catalysts. However, further deposition under these conditions leads to very few tubelike features accompanied by a lot of disorder. The presence of a substrate that limits diffusion channels may lead to disordered C accumulation after precipitation and suppress growth of high quality SWNT.

In summary, self-organization and evolution of a carbide SL during C deposition on Mo (111) have been studied. The ordering is energetically driven, such that strain in the system determines spacing of the SL and size of the carbide nanocrystals. Surface diffusion processes have been examined, and the effective activation energy is determined to be 0.7 eV. The length scale of the SL appears to control the size and spacing of C precipitates leading to a possible mechanism for nucleation of SWNT. From a wider perspective, this work demonstrates that nanoscale phenomena can be tuned and studied using tailored epitaxial processes.

This work was supported in part by ONR/MURI N00014-98-1-0597 and NSF DMR-9703419 and 0108605.

*Email address: ftsui@physics.unc.edu

[1] S. Iijima, Nature (London) **354**, 56 (1991).
[2] S. Iijima and T. Ichihashi, Nature (London) **363**, 603 (1993).
[3] D. S. Bethune *et al.,* Nature (London) **363**, 605 (1993).
[4] A. G. Rinzler *et al.,* Appl. Phys. A **67**, 29 (1998).
[5] L. C. Qin and S. Iijima, Mater. Lett. **30**, 311 (1997).
[6] H. Dai *et al.,* Chem. Phys. Lett. **260**, 471 (1996).
[7] P. A. Ryan and F. Tsui, Appl. Phys. Lett. **75**, 3796 (1999).
[8] K. Raghavachari and J. S. Binkley, J. Chem. Phys. **87**, 2191 (1987); C. H. Xu *et al.,* Phys. Rev. B **47**, 9878 (1993); R. O. Jones, J. Chem. Phys. **110**, 5189 (1999).
[9] D. Bergner, in *Diffusion in Metals and Alloys,* edited by F. J. Kedves and D. L. Beke (Trans Tech Publications, Switzerland, 1983), p. 223.
[10] At a later stage of coarsening, RHEED intensity of Mo is too weak for d-spacing measurements.
[11] For example, Ag on Ru (0001), K. Pohl *et al.,* Nature (London) **397**, 238 (1999).
[12] F. Liu, A. H. Li, and M. G. Lagally, Phys. Rev. Lett. **87**, 126103 (2001).
[13] *Powder Diffraction File,* edited by W. F. McClune (International Centre for Diffraction Data, Pennsylvania, 1989).
[14] E. Parthé, Österreich. Chem. Ztg. **56**, 153 (1955).